AIAA 92-2755
Design Trade-Offs For Homing Missiles

Allen Spencer
Delta Research, Inc.
Huntsville, AL

William Moore
Mevatec, Inc.
Huntsville, AL

AIAA SDIO Annual Interceptor Technology Conference
May 19-21, 1992 / Huntsville, AL

DESIGN TRADE-OFFS FOR HOMING MISSILES

Allen Spencer
Delta Research, Inc.
Huntsville, AL

William Moore
Mevatec, Inc.
Huntsville, AL

Abstract

Major design considerations, trade-offs and technology issues for future hypervelocity, anti-missile interceptors are presented in an overview format. Two classes of interceptors are considered: a low altitude interceptor using an active radar seeker for defense against tactical ballistic missiles (TBMs) and a higher altitude interceptor using a passive infra-red seeker for defense against ICBMs. Considerations are presented in the areas of mission requirements, seeker selection, aerodynamic and aerothermal environments, control systems, and guidance performance.

Introduction

A notable aspect in the design of modern homing missiles is the tremendous variety of choices afforded by new and emerging technologies. Miniature avionics, small, high thrust to weight ratio rocket motors, lightweight high throughput computers, sensitive and accurate focal plane array detectors, actively cooled seeker windows, solid state, millimeter wave RF devices and fast electro-mechanical actuators represent a few examples that give the missile designer a great deal of freedom. However, the gap between what has been integrated and tested, and what these new technologies can potentially support is wide and is growing wider. In addition, configurations which are optimum for a particular mission requirement are largely unknown. These factors introduce uncertainty into preliminary designs and make the selection of subsystem components difficult.

Integrating state-of-the-art interceptor technologies into candidate systems is both time consuming and costly. It requires the support of analysts in propulsion, aerodynamics, seeker design, power systems, inertial instrumentation, data and signal processing, flight dynamics and control, and guidance software and hardware. Many different combinations are possible that achieve a given performance goal requiring the evaluation of a number of candidate interceptor designs. The objective is to develop designs which are balanced in terms of subsystem requirements and are robust to the uncertainties of use in battle. The purpose of this paper is to introduce for the specialist a number of general design considerations and trade-offs which can have a major impact on the final design and performance. The subject is treated in an overview format in the interest of brevity.

General Considerations

The design process for a homing interceptor begins with the definition of a mission or defended area, the threat targets, and the desired probability of intercept or lethality. These quantities are then used to derive the required miss distance. The fundamental measures of performance for the interceptor are the statistical miss distance and the divert distance achievable against a given target. Therefore, these quantities will have the greatest influence on the final vehicle and component designs. The systems engineer or guidance engineer must derive error budgets and specifications for each of the major subsystems including the seeker, the IMU, the controls and guidance processor. This process is illustrated in Figure 1.

Each error source and contributor to miss distance must be studied and balanced among the various subsystems before important hardware decisions are made. Component specialists are then tasked to design hardware which meets the derived performance specifications and mass allocations. Sensitivity studies identify the major subsystem performance and mass trends which are then communicated back to the systems engineer who must rebalance and reconfigure the vehicle to give the best overall performance without overstressing a particular component. In this way an interactive process is established that will yield an optimal vehicle design that satisfies all the requirements and the government customer.

Several significant trends for anti-missile defense interceptors have appeared in the last several years. These include smaller size and lighter mass components, increased homing accuracy and use of strap-down seekers.

Perhaps the most significant recent trend in interceptor missiles is toward small, compact, lightweight configurations. This is made possible due to research and development of enabling technologies by the Strategic Defense Initiative and its supporting agencies. A small, light interceptor is desired to reduce the handling, transportation and deployment cost and

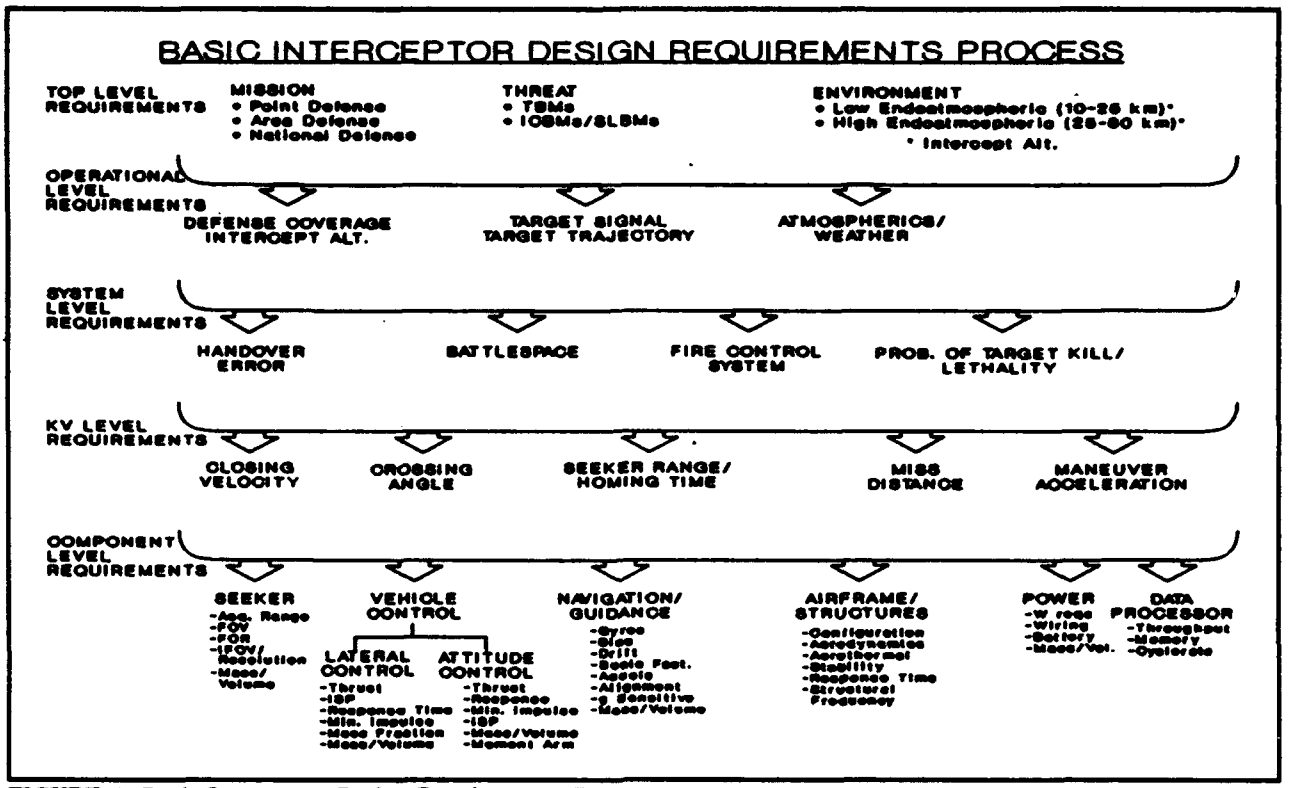

FIGURE 1 Basic Interceptor Design Requirements Process

the cost of the axial propulsion booster required to deliver the guidance equipment payload to the intercept location.

One method of reducing the size and mass of the interceptor during the homing phase is to stage the guidance and control section off the booster propulsion to leave a "kill vehicle" (KV) which contains all functions necessary to acquire, track, home on and kill a target. Without the mass burden of a spent rocket motor the KV control subsystems and structural requirements can be reduced. Another method to achieve a small KV is to require that the guidance accuracy support a direct impact of the KV with the target missile body. This eliminates the need for a heavy warhead resulting in a lighter, less complex and safer KV design. There is a limit to how small a kill vehicle can be made and still remain an effective weapon. Obviously, as you reduce the size of the KV airframe, the available area for the seeker collecting aperture is also reduced thereby decreasing the resulting seeker resolution, angular accuracy, and acquisition range. Since the miss distance performance is a strong function of the seeker angular measurement accuracy, there will be a lower limit on KV diameter which constrains the design. This effect is more pronounced at RF wavelengths than for visible or IR seekers. Another consideration that sets a lower limit on KV mass is the target destruction capability or lethality. Even if a guided B-B, traveling at extreme velocities, could be made to hit an RV target, it may not destroy or disrupt it enough to prevent warhead detonation or dispersal of chemical agents. Scientists exploring this aspect of the defense system have determined that there is a minimum mass-on-target requirement as well as a minimum kinetic energy of impact requirement for a KV to have a high probability of completely destroying its target. Another significant trend is for increased speed which decreases the flyout time to the intercept location. This reduces the range requirements on fire control sensors and still allows large defense coverage. The high speed creates a number of aerodynamic and aerothermodynamic problems.

To summarize the above points, smaller, lighter, more compact KVs are desired, but there are practical and operational limits which may constrain the minimum size and maximum speed over and above the theoretically smallest and fastest homing package that can be achieved using the latest technologies.

Low Altitude Theater Missile Defense

Assume that mission analysis has determined a requirement for intercepting tactical ballistic missiles at 10 km altitude and that the interceptor should be traveling at 1.5 to 2.0 km/s to enforce the defense timeline constraints.

Seeker

Intercepts at 10 km altitude imply that the seeker will begin operation at altitudes of 5 to 8 km. Therefore, the presence of rain and snow must be considered in the choice of seeker type. Active RF seekers are less affected by target signal attenuation and interference due to severe weather conditions than are passive infra-red seekers. The desire for good resolution with compact size and reasonable weight narrows the frequency choices to 35 and 94 GHz. Both of these frequencies suffer from some amount of atmospheric attenuation due to water vapor and rain with 94 GHz experiencing the greater level of attenuation. However, a 94 GHz seeker will have better angular measurement accuracy for a given antenna diameter. These considerations are summarized in Table 1.

Table 1 RF Seeker Frequency Considerations

GHz	Angular Accuracy	Weather Effects	Technology Maturity
35	Less	Less Affected	Demonstrated
94	Better	Greater Attenuation	Less Mature

The field of regard (FOR) or maximum scan angle, shown in Figure 2, is an important requirement for the seeker design. This parameter is primarily determined by the maximum engagement crossing angle but is also affected by the IMU flyout errors, the target position uncertainty at the time of acquisition, and the vehicle maximum angle of attack.

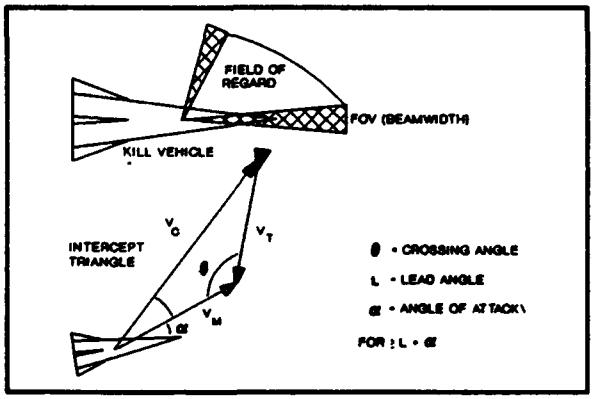

FIGURE 2 Seeker Field of Regard

Figure 3 shows the FOR requirement as a function of the intercept range for an example target. The FOR is

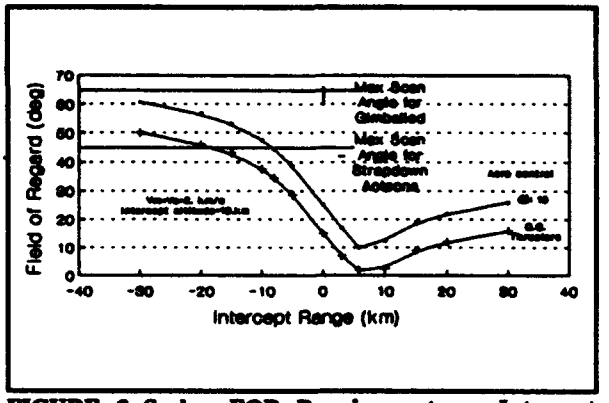

FIGURE 3 Seeker FOR Requirements vs Intercept Range

greater for engagements which are to the rear of the interceptor launch site where forward is toward the target launch site. Also shown on this figure are practical scan angle limitations for gimballed and strapdown antenna systems. Strapdown radar antennas suffer a large amount of beam shape degradation with an associated loss of accuracy as the beam is scanned beyond 45° to the antenna face. Therefore, rear intercept ranges will be limited to about 10 km for kill vehicles using strapdown seekers and employing aerodynamic maneuver control. If rocket motors, arranged about the vehicle center of gravity, can be used for the homing maneuvers then any angle of attack will be small and more rear defense coverage can be achieved.

Strapdown seekers are desired because they eliminate costly, heavy gimbal sets and are, therefore, more accurate, rugged and compact. However, there are also drawbacks such as the one mentioned above and the fact that strapdown seeker guidance systems are more sensitive to certain seeker errors including scale factor, quantization errors, and vehicle structural resonances. Strapdown seekers also require greater IMU gyro resolution and bandwidth.

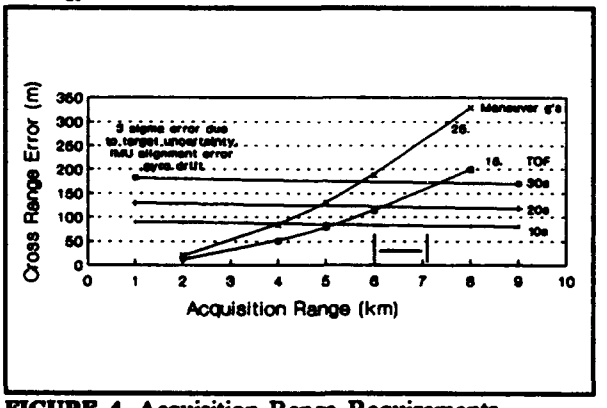

FIGURE 4 Acquisition Range Requirements

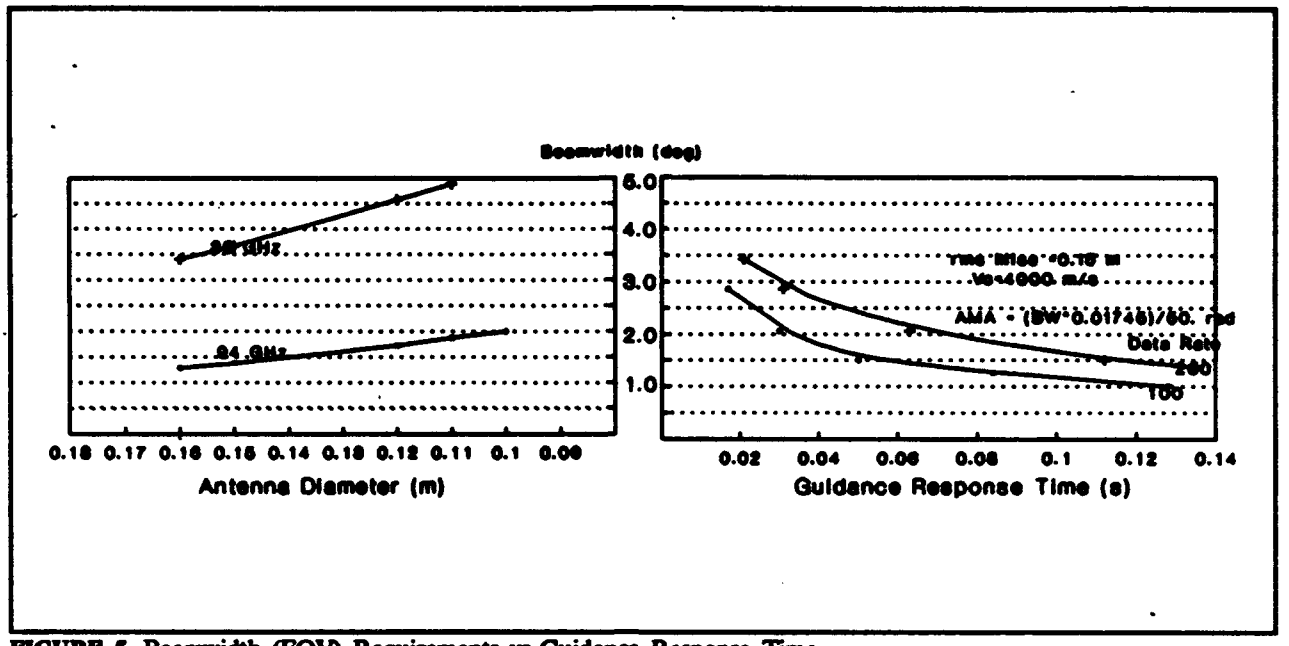

FIGURE 5 Beamwidth (FOV) Requirements vs Guidance Response Time

Figure 4 shows the relationship between the seeker acquisition range, the vehicle maneuver capability and the cross range error or initial miss distance that can be removed during homing. Three levels of maximum initial error are shown corresponding to interceptor flight times of 10, 20 and 30 seconds. This error is due primarily to the target position uncertainly and to the KV's IMU gyro misalignment error and random drift rate. The vehicle maneuver curves assume a proportional navigation gain of 3.0. This analysis indicates that the seeker should have an acquisition range of 6.0 to 7.0 km.

Another major requirement for the seeker design is the angular measurement accuracy (AMA). This parameter, largely a function of the signal-to-noise ratio (S/N) and the effective beamwidth, is the primary determinant of miss distance capability and so it must be analyzed in detail so that the desired P_{hit} can be achieved. Figure 5 presents a trade-off of beamwidth versus the guidance and control system closed loop response time to achieve a rms miss distance of 0.15m. The required antenna diameter for 35 GHz and 94 GHz is also shown. This type of analysis is used to balance the seeker accuracy with the response time of the guidance filter plus the control subsystem. It is seen from this figure that a 94 GHz seeker with an antenna diameter of .15m (AMA ≈ 0.4mrad) and operating at a 100 Hz data rate will require a guidance and control subsystem capable of achieving a 50 to 60msec response time. If the seeker can deliver a 200 Hz data rate then the response time can be relaxed to about 100 msec.

The selection of radome shape and material is integral with the selection of wavelength and antenna diameter. A low drag nose shape with large fineness ratio (~3) will also have large radome boresight error slopes that tend to destabilize the control subsystem and degrade the miss distance performance. This is shown in Figure 6 for silicon nitride and slip cast fused silica materials. Lower fineness ratios (1.5 to 2.0) combined with 10 to 20% nose blunting (a hemispherical nose cap) can significantly reduce the heat transfer rate to the radome and reduce the mean boresight error.

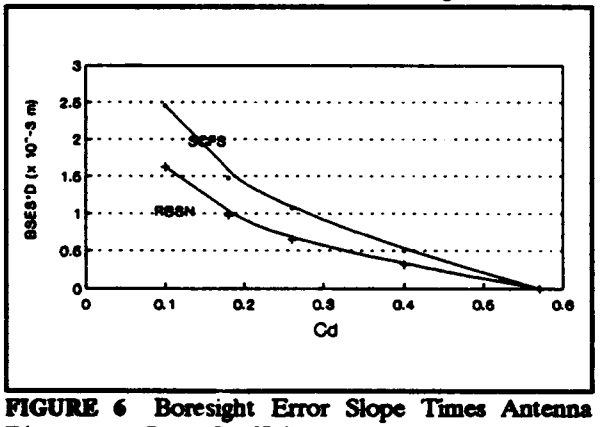

FIGURE 6 Boresight Error Slope Times Antenna Diameter vs Drag Coefficient

There are, of course, many additional trade-offs and error sources to be considered in the design of the seeker with the above examples serving to illustrate some of the basic principles and considerations involved.

Controls Subsystem

The fundamental measures of performance for a homing missile are the total maneuver capability and the achievable miss distance. Clearly, the control subsystem(s) will influence both these quantities. The maneuver capability, usually measured in term of lateral g's, determines the maximum initial miss distance that can be removed during the homing phase and influences the miss distance against a maneuvering target. The miss distance is a strong function of the overall guidance response time, which in turn is a function of the control subsystem response. Therefore, the total control authority and speed of response afforded by a particular design will determine the miss distance performance.

The control authority required is determined by several contributions: midcourse corrections due to target updates, homing divert due to initial heading error, target maneuver during homing, and spurious commands due to noise. The total amount of control authority in terms of ΔV or in g-seconds can be estimated by the relation

$$\text{CONTROL AUTHORITY } (\Delta V \text{ in ft/s or g-seconds}) = \frac{2D_{mc}}{(T_u - T_g)} + \frac{G}{G-1}\left[\frac{M_0}{T_h} + \frac{\zeta_T T_h}{2}\right] \quad (1)$$

where D_{mc} = midcourse correction
M_0 = initial miss distance to be removed
ζ_t = target maneuver level
T_h = homing time (T = 0 at intercept)
T_u = time of midcourse update (referenced to intercept time)
G = guidance gain.

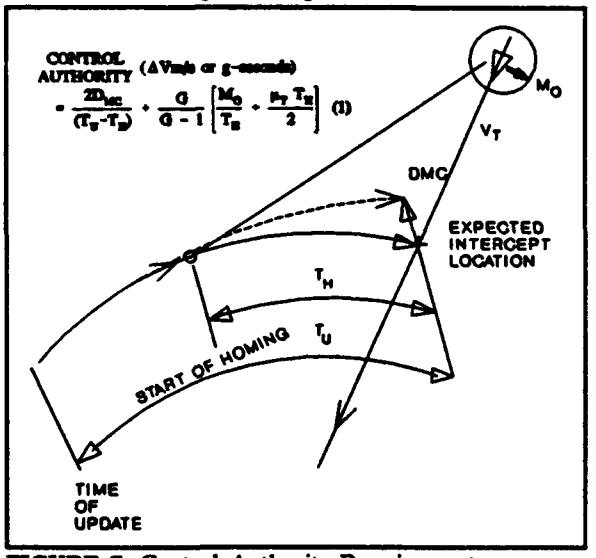

FIGURE 7 Control Authority Requirements

The geometry is illustrated in Figure 7. Example KV maneuver level and control authority trades are presented in Figure 8 as a function of the homing time for target maneuver levels of zero and six g's. Larger values of guidance gain result in higher g level requirements for the kill vehicle but reduce the required control authority.

Aerodynamic control surfaces are the standard method for controlling endoatmospheric missiles. However, certain performance and technological limitations of aero-control surfaces provide the motivation for the use of reaction thrust controls. Aerodynamic controls provide good maneuver stamina for long range flyouts and midcourse maneuvers. However, reaction thrust controls can reduce the guidance response time, thereby improving performance against target maneuvers and seeker noise.

Reaction thrust control uses liquid or solid rocket motors arranged longitudinally, to effect changes in a missile's flight path heading. This can be accomplished by placing the thrusters about the missile center of gravity (c.g.) to provide direct divert capability or by placing the thrusters either fore or aft of the c.g. to cause a rapid rotation of the missile airframe. Lateral maneuver forces then result from the aerodynamic interaction of the missile body due to the induced angle of attack. Figure 9 summarizes considerations for the selection of the control thruster location.

C.g. thrusters offer the fastest response but require a large thrust capability to directly provide a maneuver. Aft thrusters rotate the missile body to provide angle-of-attack but the thrust is opposite to the desired maneuver direction. Forward thrusters also rotate the airframe to provide an angle-of-attack and have the benefit that the thruster force is in the desired maneuver direction. In addition, forward location of the thrusters usually provides a longer torque moment arm than aft locations since the c.g. of most missile configurations will be closer to the aft end of the missile. Packaging considerations usually favor aft thruster configurations.

The combination of control types may be optimum for many applications. For example, aero-control surfaces or attitude control thrusters can be used for divert early in the homing phase with c.g. thrusters used in the final few tenths of a second to improve accuracy and to reduce sensitivity to parasitic guidance effects such as the radome boresight error slope.

The basic equations for determining the control force and impulse requirements are shown in Figure 10. In order to develop control subsystem requirements and performance estimates a

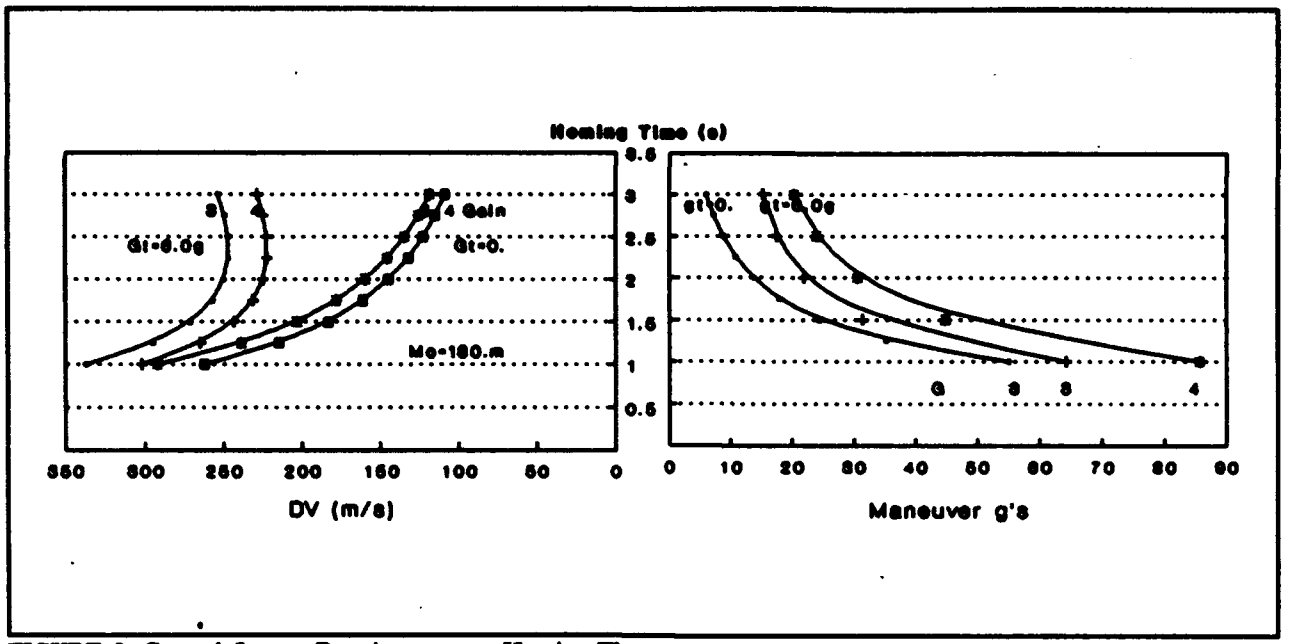

FIGURE 8 Control System Requirements vs Homing Time

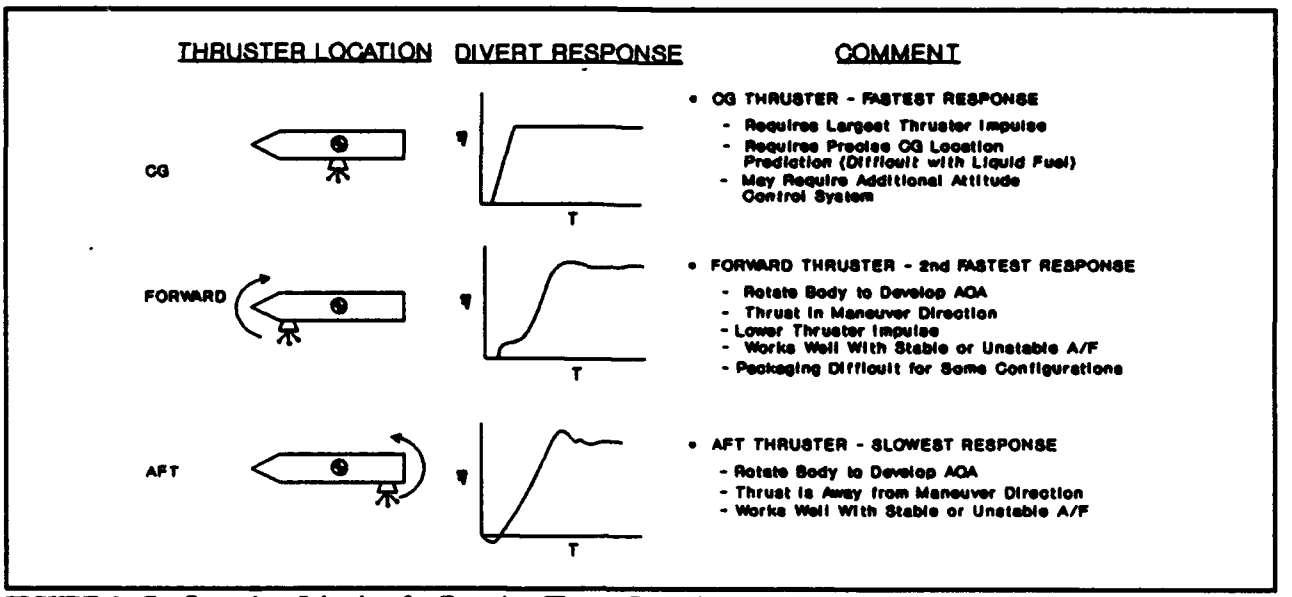

FIGURE 9 Configuration Selection for Reaction Thrust Control

representative KV configuration is defined as a baseline for study and trade-offs. The baseline KV parameters are:

mass	~ 20 kg	ℓc.g.	~ .4 m
length	~ 0.8 m	ℓc.p.	~ .45 m
diameter	~ 0.18 m	$I_{yy} = I_{zz} \sim 1.8$ kg-m^2	
α_{max}	≤ 15°	$I_{xx} = .15$ kg-m^2	

The required control force as a function of the ratio $\ell c/\ell sm$ is given in Figure 11 where the derived maneuver level is taken as 25 g. The total control impulse requirement for a 1.5 to 2.0 sec homing time is also shown in Figure 11. Moving the thrusters forward of the c.g. just 0.05 m ($\ell c/\ell sm = 1$) reduces the control system requirements by one half compared to a c.g. arrangement. It is also seen from these results that a KV design employing c.g. thrusters would require 75 kN-s of stored impulse ($\Delta V \approx 375$ m/s) to deliver a 25 g maneuver over the homing time. The response time of the thrusters can be from 5 to 20 msec. This configuration would therefore deliver the minimum miss distance. Thrusters at other locations require some of the maneuver to be delivered by airframe rotation which introduces an additional lag time into the guidance response for any given maneuver level.

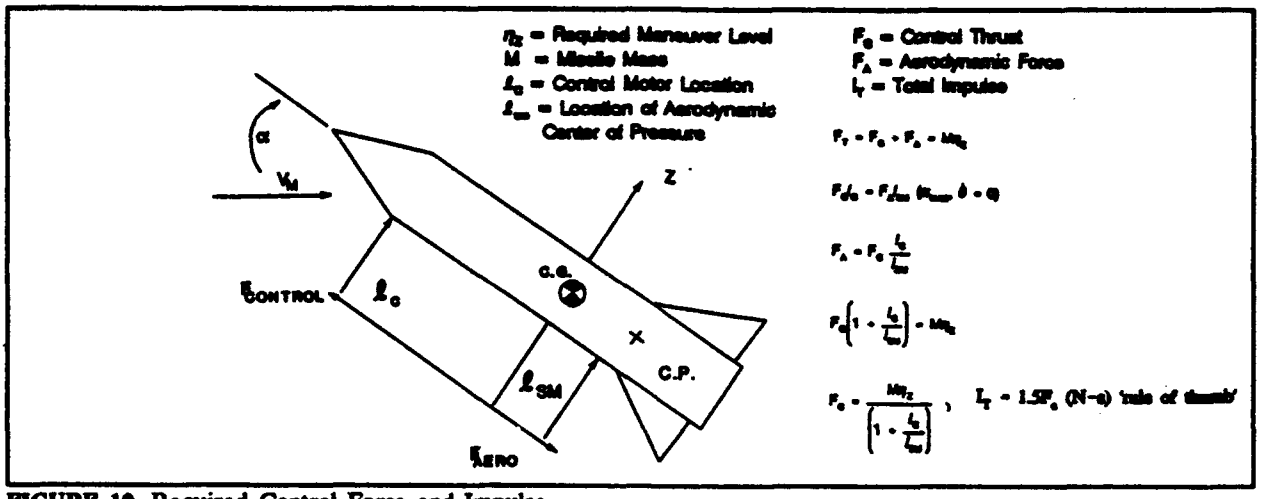

FIGURE 10 Required Control Force and Impulse

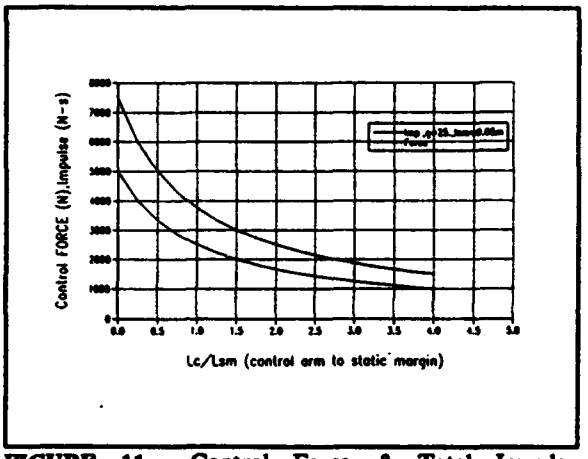

FIGURE 11 Control Force & Total Impulse Requirements vs L_c/L_{sm}

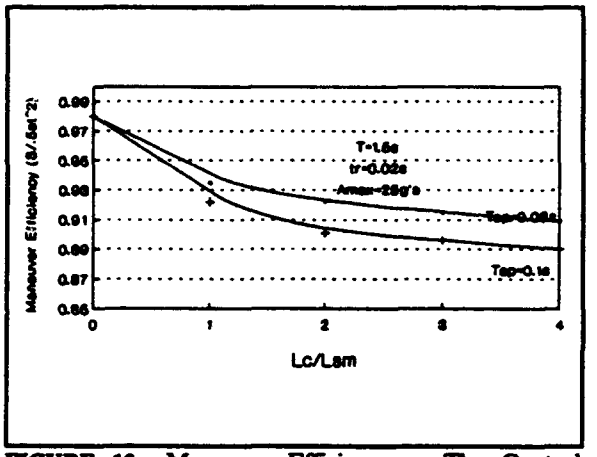

FIGURE 12 Maneuver Efficiency vs The Control Position Ratio ℓ_c/ℓ_{sm} (Forward Thrusters)

One measure of performance for the control subsystem is the maneuver efficiency defined as the ratio of lateral divert distance achieved to the maximum theoretical value given by $1/2aT_H^2$. This is shown graphically in Figure 12 for the example KV design and two autopilot response times. The relationship between thruster location, ℓc with respect to the c.g., and the miss distance is presented in Figure 13 for three closed loop autopilot plus airframe response times. It is seen that no substantial increase in miss distance is realized for ℓc greater than about .1m, however, the control impulse requirement continues to benefit from larger ℓc until about .15m, ($\ell c/\ell sm$ = 3) .

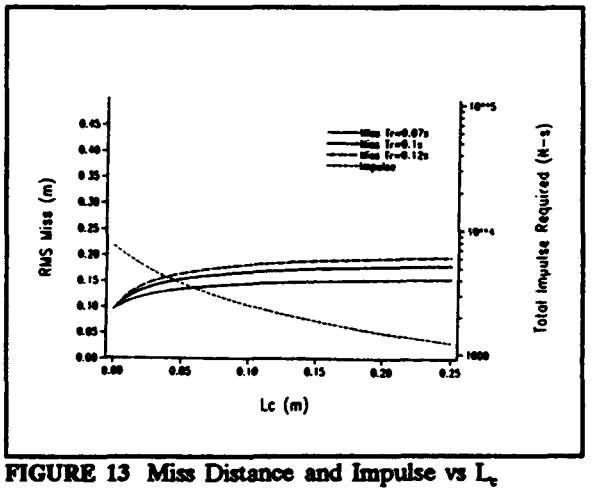

FIGURE 13 Miss Distance and Impulse vs L_c

The control subsystem mass can now be estimated for the example KV by the following:

$$M_C = \frac{I_T}{I_{sp} \bullet g \bullet \lambda} \qquad (2)$$

where I_T = the required impulse
I_{sp} = the effective fuel I_{sp} (250)
g = gravity
λ = propellant mass ratio (M_p/M_C) (0.2).

Taking the required impulse as 1666 N•s the propulsive control subsystem mass estimate becomes 3.4 kg.

Guidance

The guidance function cannot strictly be assigned to a particular component since it is the interaction of a number of vehicle subsystems which create homing guidance. The seeker must measure the target signal to extract information which is converted into an acceleration command by the guidance law algorithms. The autopilot software then translates the output from the guidance law calculations into control actuator commands which effect a change to the vehicle motion. What is most often termed "guidance" is the combination of the noise filter/estimator with a guidance policy or guidance law.

TABLE 2 Missile Guidance Law Comparison

GUIDANCE LAW	FORM	GUIDANCE GAIN
Proportional Guidance	$GV_c\dot{\lambda}$	CONSTANT - 3
Augumented Proportional Guidance	$GV_c\dot{\lambda} + \alpha_1$	CONSTANT - 3
Optimal Linear Guidance with Target Maneuvers	$C_1\hat{X}_T + C_2\hat{\dot{X}}$	$C_1 = G/T_{go}^2$, $C_2 = G/T_{go}$ LIM • G = 3 $T_{go} \rightarrow 0$
Optimal Linear Guidance w/Target Maneuver & Autopilot Dynamics	$C_1\hat{X}_T + C_2\hat{\dot{X}}_T + C_3\hat{\ddot{X}}_T + C\eta_M$	$C_3 = G\left[\frac{e^{-\lambda_t T_{go}} + \lambda_t T_{go} - 1}{\lambda_t^2 T_{go}^2}\right]$ $C_4 = -C_3$ G increases to ~ 10 As $T_{go} \rightarrow 0$ G - function of autopilot response and T_{go}

The filter of choice for modern missiles is the Extended Kalman Filter which attempts to extract a smoothed estimate of the target state in a non-rotating coordinate system based on seeker measurements corrupted by vehicle body motions and various noise and bias errors. A discussion of the theory and sensitivities for the selection of the guidance filter is beyond the scope of this paper, however, it is an integral and critical aspect for successful homing.

Guidance law policy is clearly an important area of study for modern homing missiles. At the extremely high closing velocities and large engagement crossing angles expected for anti-missile intercepts the traditional proportional navigation (PN) law may be inadequate. Augmented proportional navigation (APN) introduces a compensation term to PN which accounts for target acceleration normal to the relative line of sight. A number of "modern" guidance laws have been derived using the principles of linear optimal stochastic control theory in an attempt to improve miss distance performance over the classical PN laws. Basically these guidance laws differ in the formulation of the guidance gain. A comparison is given in Table 2.

Optimal guidance laws generally provide improved performance over PN or APN against maneuvering targets and with control non-linearities such as saturation and bang-bang operations. The increased complexity of these laws also makes them very sensitive to target assumptions, boresight error slope, and to estimation errors in time-to-go. The choice of Kalman filter and guidance law implementation would become the subject of a detailed study once the final KV hardware design is completed using detailed six degree-of-freedom dynamical simulations.

High Altitude ICBM Defense

It is assumed that mission analysis has determined that a very high speed endoatmospheric missile is needed to perform engagements from 25 to 65 km in altitude. Missile speed at target acquisition time is required to be about 3.0 to 4.0 km/s to enforce a large protective coverage area.

Seeker

The desire for a small, compact, low mass kill vehicle dictates that a hit-to-kill, no-warhead approach be pursued. This implies that very accurate seeker, guidance and control subsystems will be needed.

As the ICBM reentry vehicle (RV) enters the atmosphere it will heat up providing significant radiation for a passive infra-red seeker. Figure 14 shows a typical radiant intensity profile as a function of altitude.

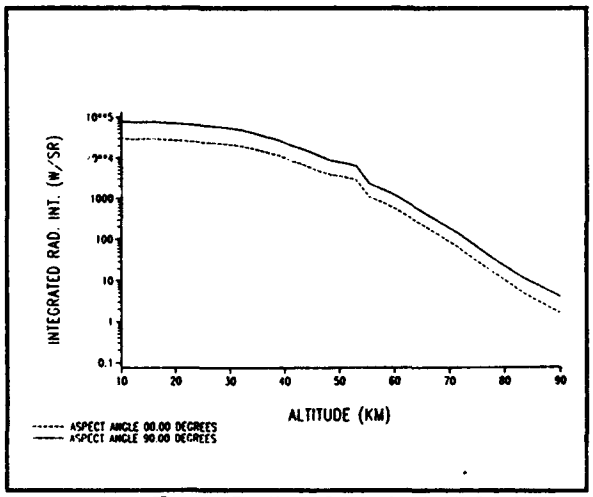

FIGURE 14 Target Radiant Intensity in 3-5μ Band

The high speed flight of the KV will generate significant aerothermal heating of the seeker window and outer structure. This is more critical at lower altitudes where the air density is greater. The shock wave and heated boundary layer will disrupt and attenuate the target signal and irradiation from the heated seeker window material itself will reduce the target contrast. At low altitudes some sort of cooling mechanism must be provided for the window for material survival and to prevent a saturation of the detectors due to window emission. The cooling scheme may involve either external or internal cooling fluids over the window or an edge cooling approach using a heat pipe/heat sink apparatus. The use of cooling fluid increases the target signal disruption.

All of the above phenomena have been termed "Aero-optical (AO) effects". The study of these effects and their interaction with the seeker operations and with the guidance implementation are major areas of research and development within the Strategic Defense Initiative. The AO effects can be separated into image boresight shifts or boresight error (BSE), jitter or image dancing, blur or image spreading and attenuation or reduction in the target intensity. This is illustrated in Figure 15. All of these effects degrade the miss distance performance. The table indicates the relative contribution from each source to the total. It is seen that if ways can be found to eliminate the requirement for external cooling fluid then the AO effects can be reduced by an order of magnitude.

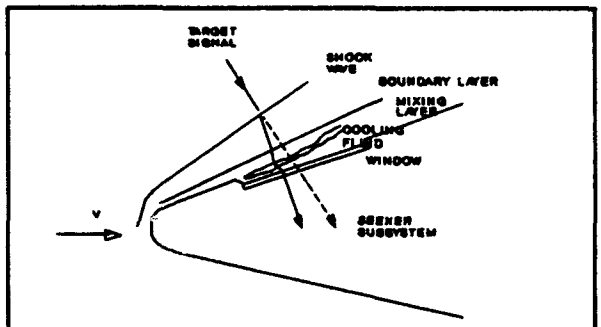

SOURCE OF AO EFFECT	% OF TOTAL EFFECT BSE	JITTER	BLUR	ATTEN.
BOW SHOCK	80%	<1%	.5%	.5%
BOUNDARY LAYER	<1%	10%	5%	10%
COOLANT LAYER	20%	<1%	<1%	<1%
MIXING LAYER	15%	90%	90%	90%
WINDOW	10%	<1%	5%	<1%

FIGURE 15 Aero-Optical Effects

The bow shock is the major source of BSE, but this effect can be predicted and therefore compensated in the seeker signal and data processing. The other effects are not well understood. The usual approach is to estimate their peak values at different altitudes and balance the miss distance effects by increasing the overall angular accuracy requirement of the seeker optical components.

The seeker IFOV, the optical "beamwidth" given approximately by λ/D, is perhaps the most important parameter for the seeker design. Its value determines the angular measurement accuracy, the volume of space that can be observed without scanning or steering, the acquisition range for a given detector sensitivity and the image resolution for extended targets. A small IFOV is desired to improve range performance, angular accuracy and resolution and to decrease the amount of collected background radiation from the window and boundary layer. A small IFOV will require a moveable scanning element so that the IFOV can be steered to search for the target over the seeker field of regard (refer to Figure 2) and for line-of-sight stabilization.

A fundamental trade-off for the seeker and vehicle design is shown in Figure 16 where the required angular accuracy and closed loop guidance response time are balanced for a given rms miss distance, taken here as 0.1m.

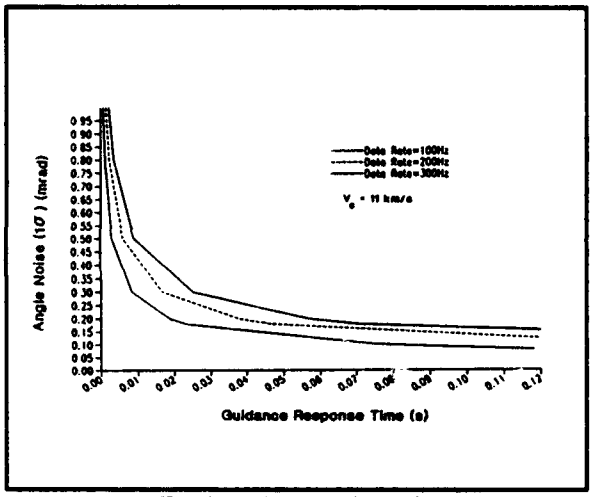

FIGURE 16 Total Seeker Angle Noise vs Guidance Response Time for Constant Miss

The angular measurement noise is composed of seeker measurement noise at high S/N and jitter from AO effects and structural vibrations. Combinations of angle noise and response time which fall on or below these curves will support the miss distance requirement. However, it is best to choose values which are near the nee of these curves to provide robustness to hardware and environmental uncertainties. A total angle noise budget of 0.2 mrad (1σ) and a guidance response time of less than 30 msec appear reasonable for this mission. For preliminary design purposes one half the total angle noise budget can be ascribed to the seeker and its processing algorithms. Taking the tracking accuracy of the seeker as IFOV/2 implies that the IFOV should be between 100 and 200 mrad. The seeker collecting aperture D becomes about 3.5 cm. A more detailed discussion of the miss distance due to seeker noise is presented in the Appendix.

In order to provide long range intercepts with side and rear coverage the KV must support acute engagement geometries. The engagement crossing angle is defined by

$$\theta = \cos^{-1}\left(\frac{\bar{V}_T \cdot \bar{V}_M}{V_T V_M}\right) \qquad (3)$$

This is illustrated in Figure 17. Small crossing angles imply that a very large seeker FOR would be required if the KV must fly at zero angle of attack (α). One approach to relieve the stressing FOR requirements allows the KV to orient itself near the line-of-sight, or to fly at a constant trim angle of attack as shown in the figure. Clearly, this approach is only applicable at high altitudes where the aerodynamic lift forces will be small. Figure 18 shows the maximum trim α and relative velocity as a function of the crossing angle. The resulting drag acceleration of a representative KV design flying at a trim angle of attack of 90° is presented in Figure 19 which indicated that this concept is feasible above 50 km altitude. There is another advantage to orienting the vehicle center line near the line-of-sight direction. The most efficient use of the divert control thrusters is normal to the line-of-sight. Therefore, a greater initial miss distance can be removed for the smaller crossing angles with this concept.

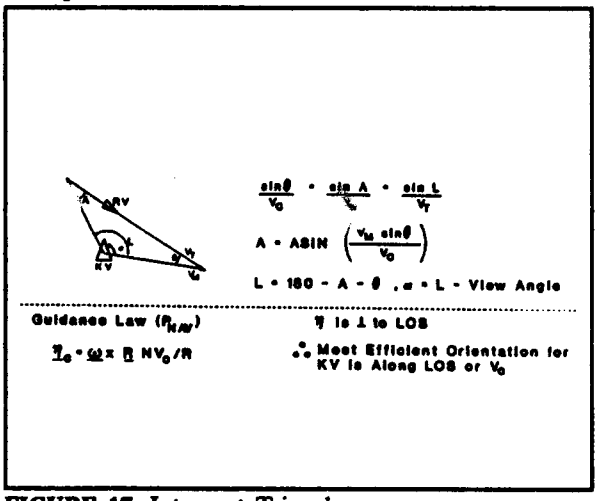

FIGURE 17 Intercept Triangle

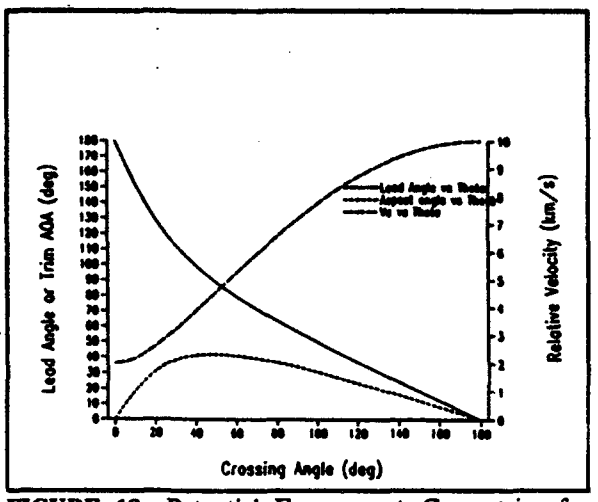

FIGURE 18 Potential Engagement Geometries for the High Altitude Interceptor

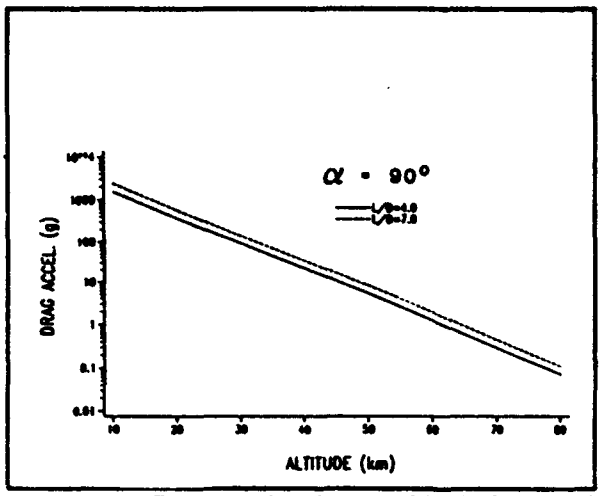

FIGURE 19 Drag Acceleration vs Altitude for α=90°

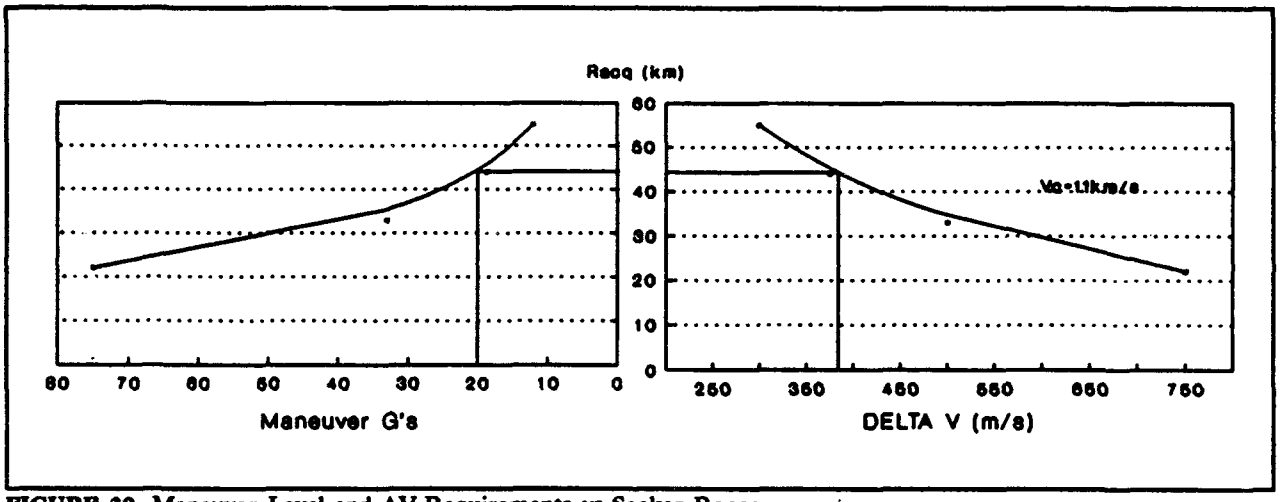

FIGURE 20 Maneuver Level and ΔV Requirements vs Seeker Range

Controls Subsystem

Homing operations at altitudes above 25 km require the use of rocket thrusters placed about the vehicle c.g. The major requirements which size the propulsive control subsystem are shown as a function of seeker acquisition range in Figure 20. Longer acquisition range allows more time to remove the initial heading error but also requires greater detector sensitivity and dynamic signal range. In addition, a longer homing time will require more window cooling fluid which increases the mass.

The divert control subsystem mass can be estimated as follows. The ΔV requirement was shown to be about 400m/s. The propellant mass is given by,

$$M_p = \Delta V M_o / g I_{sp} \qquad (4)$$

where M_p = propellant mass
I_{sp} = specific impulse
M_o = KV initial mass.

The subsystem mass fraction, λ_{MF}, is defined as the ratio of propellant mass to total control subsystem mass i.e., $\lambda_{MF} = M_p/M_c$. Therefore,

$$M_C = M_p/\lambda_{MF} = \Delta V M_o / g I_{sp} \lambda_{MF} \qquad (5)$$

The divert system mass as a function of λ_{MF} is given in Figure 21 for a propellant I_{sp} of 250s and 280s. The KV initial mass is taken as 20 kg.

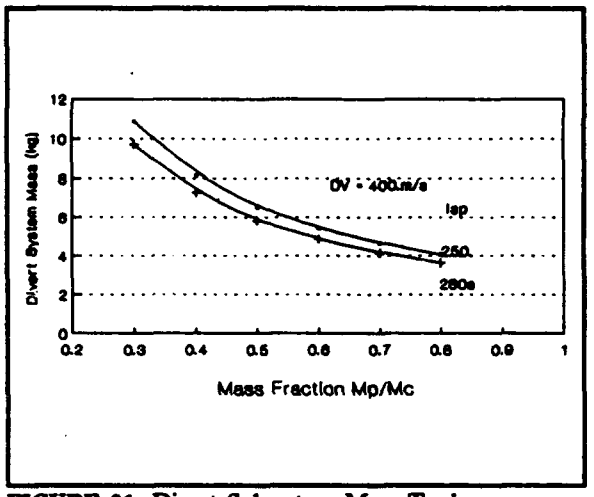

FIGURE 21 Divert Subsystem Mass Trades

Another important parameter for the divert system is the minimum impulse bit, $_{min}$. I_{min} is the product of the thrust and the minimum "on" time for the divert thruster and will have a major impact on the minimum achievable miss distance. The I_{min} can be estimated by,

$$I_{min} \approx 2M_0\sigma_{miss}/10\tau_r \qquad (6)$$

where σ_{miss} = 1 sigma miss requirement
M_0 = KV mass
τ_r = thruster response time.

Taking the 1 σ_{miss} as 0.1m and τ_r as 10 msec, the I_{min} = 40 N-S.

The attitude control subsystem (ACS) is somewhat more difficult to size, because it is used to stabilize as well as orient the airframe and is therefore dependent on autopilot bandwidth requirements. For a strapdown seeker configuration the ACS will be required to help stabilize the line-of-sight angle to the target and prevent rapid body rotations when the divert thrusters are on. For preliminary design estimates a good "rule-of-thumb" is to require the response time of the ACS thrusters to be about one half that of the divert thrusters and the I_{min} for the ACS should be 1/50 of the divert system.

Aerodynamics/Aerothermal

There is a traditional desire for interceptors to have low drag configurations. This is so the resulting slow down won't appear as a target maneuver and increase the intercept time uncertainty. However, use of the on-board accelerometers and an appropriate guidance law can compensate for even large drag values. Low drag usually implies a "sharp" nose shape. A sharp nose results in high heat transfer rates to the seeker window and aft body sections.

The heat transfer rate to the KV body is inversely proportional to the square root of the nose radius. A blunter nose, large nose radius, leaves more of the drag energy in the bow shock wave resulting in a lower energy, slow speed boundary layer. The boundary layer will be thicker, but it will have less turbulence and, therefore, less AO jitter and attenuation. More energy or pressure gradients across the shockwave will result in a greater boresight error. In addition, the lower heat transfer associated with blunt nose configurations will reduce the required mass of thermal protection materials on the aft KV sections. The advantages and disadvantages of blunt nose shapes are summarized in Table 3.

Table 3 Comparison of Blunt vs Sharp Nose Shape

	ADVANTAGES	DISADVANTAGES
BLUNT NOSE	Reduced Heat Flow	Increased Nose Wave Drag
	Lower vibration environment over window	Increased BSE contribution of shockwave
	Less turbulence in B.L.	
	Moves center of pressure aft	
	Less AO jitter	
SHARP NOSE	Lower drag	Higher heat flux in window
	Less BSE in shockwave	C.P. forward

The static stability of the airframe is an important design consideration for intercept altitudes less than 40 km. A small, static margin is desired to minimize the ACS mass and control thrust, but enough aerodynamic stability is needed so that the airframe will rotate quickly into the resultant wind direction after a c.g. thruster firing. An unstable configuration will require a larger amount of ACS fuel just to stabilize the KV in the presence of atmospheric turbulence, high altitude winds and to off-set thruster misalignment torques. If the static margin is made too large, the ACS must overcome large aerodynamic restoring forces in order to turn the vehicle. These considerations are shown notionally in Figure 22. The figure-of-merit used for the airframe is the open loop response time which is a measure of the time required for the KV to return to a zero angle-of-attack condition after a disturbance torque has occurred.

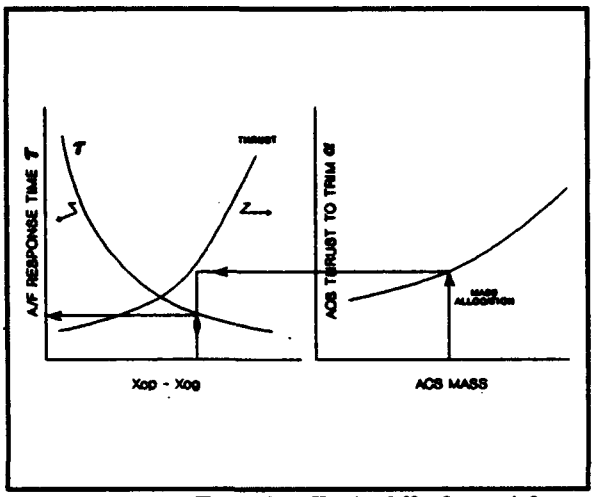

FIGURE 22 Example Trade-Off for Airframe Stability and ACS Sizing

Guidance

A number of issues exist for passive homing guidance of hypersonic KVs. The use of optimal guidance laws is desired to reduce the achievable miss distance. These laws require an explicit target state estimation and estimate of time to go. An Extended Kalman Filter (EKF) can be devised to estimate the targets inertial position and velocity using only the bearing angle information available from the seeker. These filters typically need a relatively high value for the target line-of-sight angular rate and acceleration to yield good accuracy. However, the homing guidance attempts to drive these values to zero which partially defeats any advantages. Also, the choice of guidance coordinate system is a key design parameter. The use of polar (R, AZ, EL) versus cartesian (X, Y, Z) systems is a potential area for study.

The guidance system engineer attempts to design a guidance and control policy which is robust to the various known noise and bias sources and is also insensitive to additional unknown errors which may be present. Individual component designers must attempt to minimize the sources and magnitudes of the errors within the available technology. In this way a reliable and more rugged weapon system will emerge. The major contributors to miss distance from each of the primary kill vehicle components is presented in Table 4. The relative contribution of each source to the total miss budget is also given. The seeker and guidance filter implementation will usually account for about 70% of the total miss distance.

A more detailed discussion of the miss distance sensitivities to various error sources is found in the Appendix for a representative endo-atmospheric kill vehicle.

Table 4 Major Contributors to Miss Distance (By Component/Sub System)

COMPONENT	ERROR SOURCE	RELATIVE CONTRIBUTION
SEEKER	Receiver Noise	10-20%
	Instrumentation Noise	20%
	Scale Factor/Quantization	<5%
	Boresight Errors	10-20%
	- Intrinsic	
	- Aerothermal	
GUIDANCE/ NOISE FILTER	A'Priori Noise Estimate	10-20%
	Target State Error	
	Computational Delay	
	Break Frequency (Bandwidth)	
	Model Errors	
IMU	Gyro -G Sensitive Drift	
	Gyro/Accel. Bandwidth	
CONTROLS	Saturation/Dead Bands	10%
	Response Time	
	Repeatability	
EXTERNAL	Initial Miss Distance (H.O.)	10%

NOTE: Strapdown, passive seeker, direct divert thrusters, numbers are representative of a reasonable, balanced design.

Summary

A number of general design considerations and trade-offs were presented for modern, hypersonic, endo-atmospheric interceptors. Several technical areas were covered including the seeker, aerodynamics, guidance, propulsion and controls. There are, of course, many other system and subsystem trade-offs and analyses that are required before a concept can transition into a hardware design. It is hoped that the analysis and general principles presented will aid the technology specialists in understanding the requirements and preliminary design process and the often competing considerations which are a part of a balanced kill vehicle configuration.

APPENDIX: MISS DISTANCE SENSITIVITIES

Integration and balancing of a missile system design is a formidable and complex task. Early in the design process major guidance and control parameters must be known to ensure the best possible and most efficient system. the final miss distance between a homing missile and its target is the fundamental measure of system performance and, therefore, techniques for estimating miss distance are essential to the analysis and design process.

A comprehensive pre-design analysis of a missile guidance system must include statistical disturbances such as noise, seeker and inertial errors, random initial conditions, appropriate lags and responses, and effects of significant non-linearities such as saturations and deadbands. A typical guidance and control study attempts to balance the major variables that effect the miss distance so that the best overall performance is achieved.

Monte-Carlo 6 Degree-of-Freedom (6-DOF) models are the most common means for generating miss distance statistics of non-linear systems. However, this method involves integrating comprehensive equations of motion over hundreds of repetitions and then calculating the statistics from the ensemble data. The Monte Carlo simulation method provides the highest confidence level for the non-linear guidance system evaluation. However, due to extensive a prior assumptions and approximations, and the cost in terms of computer resources and time, it is not an appropriate method for conducting preliminary design analysis.

As an alternative to complex 6-DOF simulations, Covariance Propagation is a method to statistically propagate the error (covariance) matrix of the system state variables as a function of time. This method enables access to the statistical values of the system states at any time during the computer run. The covariance propagation technique is naturally suited to trade off and parametric studies, which function more efficiently with fast turn around times and produces the required miss distance estimates in significantly fewer computer runs than the Monte Carlo method.

Implementation of the covariance propagation technique is straight forward due to the direct correlation to the classical block diagram representation of the guidance and control system. This direct correlation enables engineers to interpret and model the system easily.

Digital guidance computer representations and state estimation filters are also easily included. Non-linear functions are incorporated using statistical linearization techniques. These reasons point to the covariance propagation technique as a very viable and more efficient alternative to 6-DOFs for preliminary design and sensitivity studies.

The covariance propagation technique is based upon the representation of a dynamic, time varying system with stochastic inputs by the vector differential equation

$$\dot{\underline{X}}(t) = F(t)\underline{x}(t) + \underline{\mu}(t) \qquad \text{(A-1)}$$

Where:

$\underline{x}$ = System State Vector
$\underline{\mu}$ = White noise vector with spectral density Matrix Q
F = System dynamics Matrix.

The forcing function $\underline{\mu}$ can represent the control inputs as well as the random disturbances, and other noise sources that act on the system. The $\underline{\mu}$ functions are taken to be uncorrelated in time for ease of implementation. Random inputs dictate that the system states must be random variables.
The F Matrix contains the partial derivatives of dx/dt (x) with respect to the states $\underline{x}$. The covariance matrix $\underline{P}(t)$ of the system state variable is:

$$\underline{P}(t) = E[\underline{x}(t)\underline{x}(t)^T] \qquad \text{(A-2)}$$

E[ ] = Expectation Operator
"T" supra script = Matrix Transpose

The covariance propagation equation for the system of Equation (A-1) is:

$$\dot{\underline{P}} = F(t)\underline{P}(t) + \underline{P}(t)F(t)^T + Q(t) \qquad \text{(A-3)}$$

Equation (A-3) is also known as the linear variance equation or Riccati matrix equation. The solution of equation (A-3) by numerical integration provides the foundation for the covariance propagation technique. The diagonal elements of $\underline{P}(t)$ are the variances of the state variables. The off diagonal elements of $\underline{P}(t)$ are the covariances and represent the correlation between the different state variables.

Consequently, equation (A-3) will yield an exact solution for linear, time varying systems, whereas the Monte Carlo method yields only approximate solutions. The accuracy of the Monte Carlo method is dependent upon the number to trial samples, with an infinite number required for a precise solution. By integrating the covariance equation (A-3), a direct method of analyzing the statistical properties of $\underline{x}$ are available in a single computer run.

An interceptor missile designed for operations in the atmosphere, can assume a variety of configurations. The seeker can be gimbaled or strapdown, the air frame can be spinning or non spinning, the divert system can be aerodyne or thruster based. Noise filters, signal processors, seekers, IMUs, and derivative networks can be implemented with analog circuits, digital computers, or combinations of analog and digital components. A simplified homing guidance system block diagram is shown in Figure A-1 which depicts the representative elements of kinematics and dynamics.

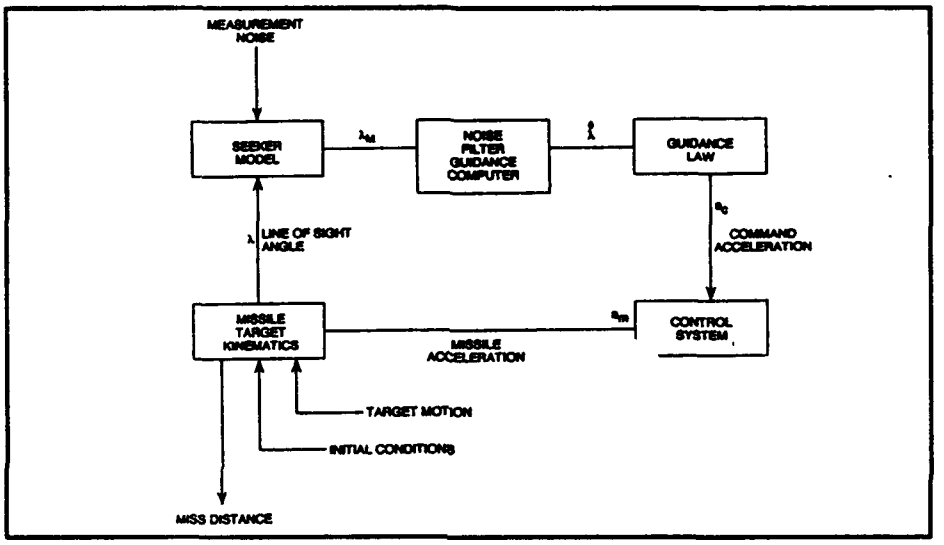

FIGURE A-1

For our purposes, we developed a model representative of the present conceptual light weight configurations currently enjoying popularity. The homing kill vehicle has strapdown passive seeker and inertial rate sensor. The control system is composed of lateral thrusters since the operational envelope consisted of altitude parameters from 15 to 80 km. The divert mechanisms are arranged in cruciform about the KV center of mass with attitude control thrusters to adjust the KV orientation.

The seeker measures the angular position of the line of sight (LOS) with respect to the seeker boresight axis, taken here to be the KV longitudinal axis. The measured quantity ϵ is added to the perceived KV inertial orientation angle θ to form the inertial LOS angle λ. The seeker measurement errors considered are instrumentation noise, BSES and jitter.

The target was modelled as a purely ballistic, non-maneuvering RV acted upon only by gravity or as a maneuvering RV with small perbutations in trajectory, but not evasive maneuvers. For relatively short homing times, the apparent acceleration of the target, due to gravity gradients between the KV and RV, will be small and is neglected.

The model for the KV-target kinematics assumes that the closing velocity (V_C) and range rate (R) will remain constant during the homing portion of the engagement. The KV acceleration is delivered normal to the LOS vector and does not contribute a change to the R.

The guidance function can be thought of as two cascaded functions; noise filtering or state estimation and the control. The filter function provides estimates of the parameters which are used in the control or guidance law. The control refers to the acceleration developed by the control system in response to commands derived from the guidance law.

The filter function is modeled in the continuous case as a simple noise filter with time constant T_N and a derivative network also with time constant T_N.

In the present study, proportional navigation is the guidance law due to its ease of implementation and use with a passive seeker use. Proportional navigation is expressed mathematically as

$$A_C = NV_C\dot{\lambda} \qquad \text{(A-4)}$$

where A_C is acceleration command normal to the LOS and in the plane defined by the V_C vector and the LOS vector. N is the guidance gain the λ is the LOS angular rate.

The thruster system is modeled as a first order lag transfer function. Divert thrusters are limited in the amount of acceleration that can be developed for a given vehicle. Therefore, acceleration saturation may occur during an engagement. This saturation represents a significant non-linearity in the system. In addition, thrust motors have a minimum thrust level. No action is taken by the control system if the command acceleration is less than the minimum throttle level. This situation is represented in the model as a dead band plus a limiter. The attitude control system is modeled as a first order lag transfer function for the actuator and a second order transfer function for the airframe response. The capability to use thrusters and aero-controls separately or in unison is also included. The model is shown in block diagram form in Figure A2.

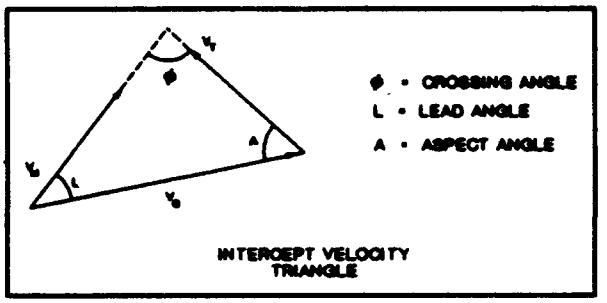

FIGURE A-3

triangle is not closed and mi ance results. The projected or virtual miss dista) is given by

$$M(t_0) = R_0^2 \dot{\lambda}_0 / V_C \qquad \text{(A-7)}$$

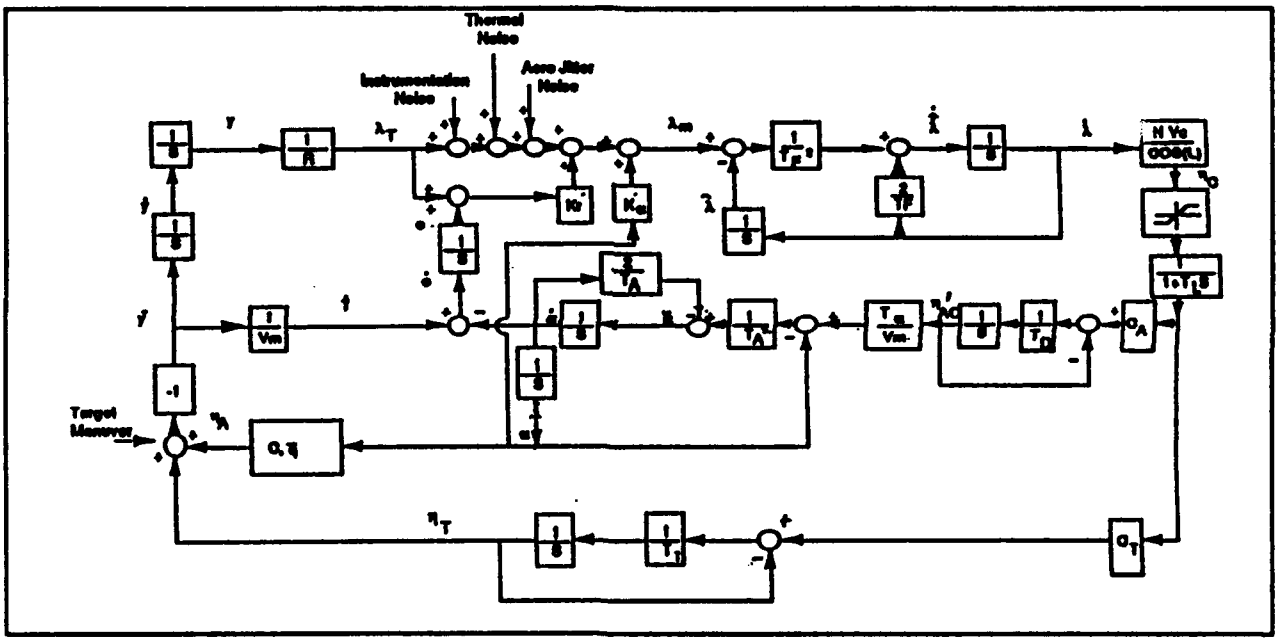

FIGURE A-2

The final miss distance is defined as the point of minimum separation between the KV and its target. The intercept geometry is shown in Figure A-3. If the KV is homing perfectly the final miss M_F is zero, and the intercept triangle is closed. The intercept condition is given as

$$V_M \sin L = V_T \sin A \qquad \text{(A-5)}$$

or

$$V_C \sin A = V_M \sin \phi \qquad \text{(A-6)}$$

If the KV is not homing perfectly then the intercept

where the subscripts indicate values at the time t_0 ($R_0 = R(t_0)$). $M(t_0)$ is the miss that would occur at the point of closest approach if no further action is taken by the KV after time t_0. The proportional navigation guidance law attempts to force intercept to occur at the point on the target's trajectory where the closest point of approach would have occurred in the absence of any homing diverts by the interceptor.

Since a CP program is completely time oriented it is important that the most accurate value of the actual homing time be obtained. Equation (A-8) is expressed in terms of the projected miss distance at acquisition and provides the most accurate homing time.

$$TF = \sqrt{R_0^2 - M_0^2 / V_c} \qquad (A\text{-}8)$$

Referring to Figure A-3, the command accelerations are normal to the LOS and in the plane defined by VC and LOS. For a non-maneuvering target this plane will not rotate in space during the engagement. A two dimensional analysis is justified where the X axis is defined along the initial LOS and the Y axis is in the intercept plane. Therefore, the kinematic model for the CP program can be restricted to the Y dimension.

MODEL PARAMETERS

Parameters that effect the miss distance performance of a homing missile guidance control system are varied and many. The examples presented are not taken from any specific interceptor/kill vehicle but are representative of the range of values that may be of interest.

The primary variables which effect the miss distance of an exoatmospheric kill vehicle are the seeker noise, the noise filter time constant, the control response time constant and the control limitations such as maximum acceleration and dead bands. For the sensitivities discussed here, the following values were chosen as representative of a KV:

Closing Velocity (VC) = 8,000 m/s

Missile Velocity (VM) = 3,500 m/s

Time of Flight (TOF) = 2-4 seconds

Filter Time Constant = .02/.04

Effective Navigation Ratio (N) = 3

Interceptor Mass (M) = 15 kg

Altitude of Operation (ALT) = 20,000 m

Computational Time Constant (TL) = .005s

Data Rate (DR) = 100, 200, 300 HERTZ

Actuator Time Constant (TD) = .01

Instrumentation Noise (SIN) = .0001 - .001 radians (1σ)

Receiver Noise (STN) = .0001 -.001 radians (1σ)

Jitter (SJN) = .001 radians

Acceleration Limit (KL) = 200 m/s^2

Dead Band (DB) = 10 m/s^2

Target Maneuver (TAR) = 10 - 100 m/s^2

Lead Angle (L) = 0 - 180

Airframe Rotational Time Constant (TA) = .1

Thruster Time Constant (TT) = .02

Boresight Error Slope (KR) = 0

Boresight Error Slope Due = 0
To Angle of Attack

Angle of Attack (ALPHA) = 0

Missile Angle (THETA) = 0

Normal Force Lift Slope (CNA) = 2

Reference Area (SR) - .031

TRADES

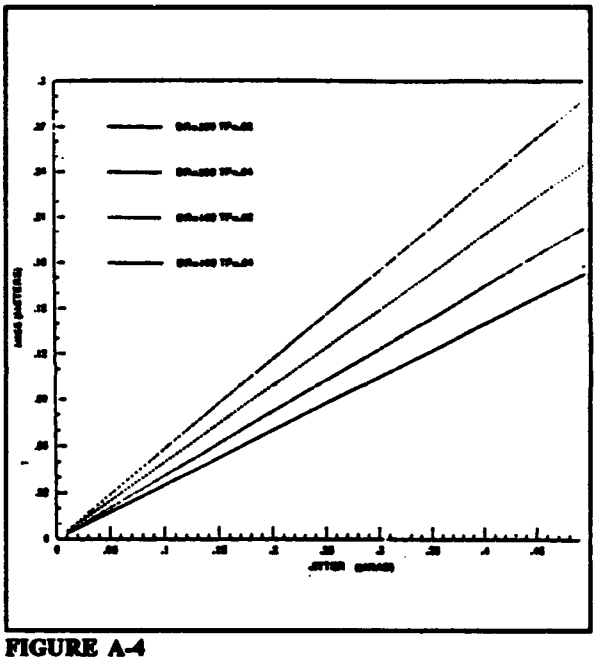

FIGURE A-4

Figures A-4 - A-9 depict the results of the analyses performed to date, expressed in the dimensions of the final miss distance (20).

Figure A-4 shows the classic trade-off of rms miss distance as a function of the seeker Jitter Noise. Variable values were used as described above with the exception of the receiver noise and the instrumentation noise which were held to 0. Four different combinations of two different data rates and two different filter time constants were used to obtain these curves. Also, a 2 second homing time was chosen as representative for this engagement. As indicated by the Figure, the miss is a strong function of the jitter noise and data rate. The filter time constants also influence the miss but not to the extent of the jitter. A choice of 100 for the data rate and .02 for the filter time constant results in a one σ miss distance of .1 meter.

Figure A-5 shows that the trade-off between miss as a function of the data rate and the filter time constant. Values for all other variables were the same as in Figure A-4, with the exception of SIN which was set at a nominal .01 mr to stimulate the system and SJN and STN which were set to zero. Increased data rates decrease the rms miss distance in this case, but as the figure depicts, little benefit is gained at data rates over 300. A data rate of 100 would meet the .1 meter 1σ miss requirements if a fast filter time constant were used. Figure A-6 shows the trade-off between miss as a function of the range dependent noise, data rate and filter time constant.

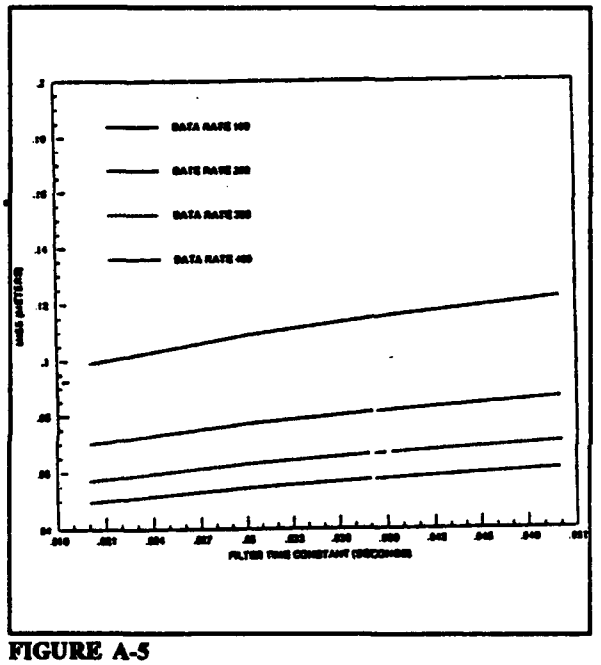

FIGURE A-5

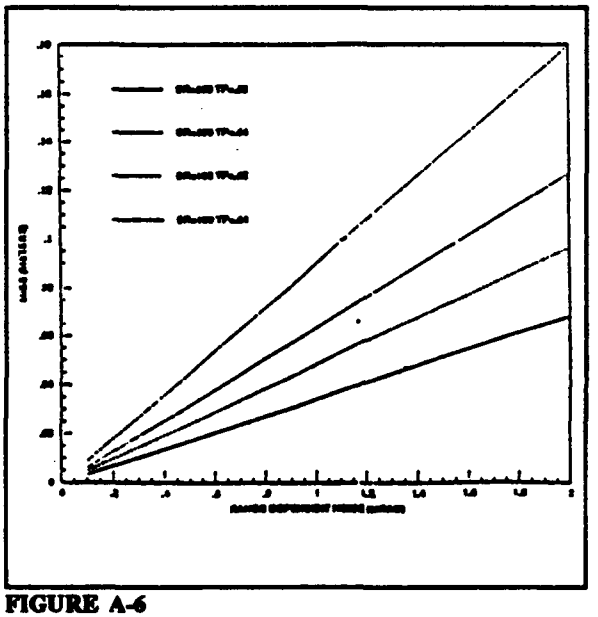

FIGURE A-6

Figure A-7 shows the trade-off between miss as a function of target maneuver, filter time constant, and the data rate. Six different combinations of the filter time constant and data rate were explored for this study. As expected, faster data rates and filter time constants provide better rms miss distance as a rule. However, for case in which the filter time constant was .02 and the data rate was 100, a counter intuitive phenomena was shown to exist. This case actually supplied better miss distances at lower values of target maneuver than cases with the same filter time constant and high data rates.

The lower data rate acted as an artificial filter to smooth the lower values of target maneuver and at the higher values of target maneuver the low data rate reduced the miss distance capability as expected. Higher data rates and faster filter time constants can improve miss distance to some degree, however, improving these factors is not sufficient against highly maneuverable targets.

Figure A-8 shows the trade-off of rms miss distance as a function of the boresight error slope, the filter time constant, and the data rate. Figure A-8 indicates that a slightly positive boresight error slope results in a reduced miss distance. However, results not shown indicate the miss reaches a minimum around .04 positive boresight error slope and increases rapidly as the boresight error slope continues to increase.

BUDGETS

Sensitivity trades performed determined characteristic limits for specific variables within the model. For the final run, the variable values which were determined to provide the least amount of final miss, thereby resulting in the best design, were combined into a single configuration. This optimized configuration was used to perform miss distance studies. A-2 second flyout was simulated determine miss distance at impact. Figure A-9 depicts the one σ miss distance plotted as a function of time. The final miss value at .5 meters. Additional runs are planned with this model to further characterize the model with the noise input optimized.

SUMMARY

A straight forward method was presented for performing preliminary miss distance sensitivity analysis and to construct a system error budget. Several numerical examples were shown indicating general trends for a representative hypervelocity homing missile using a passive seeker.

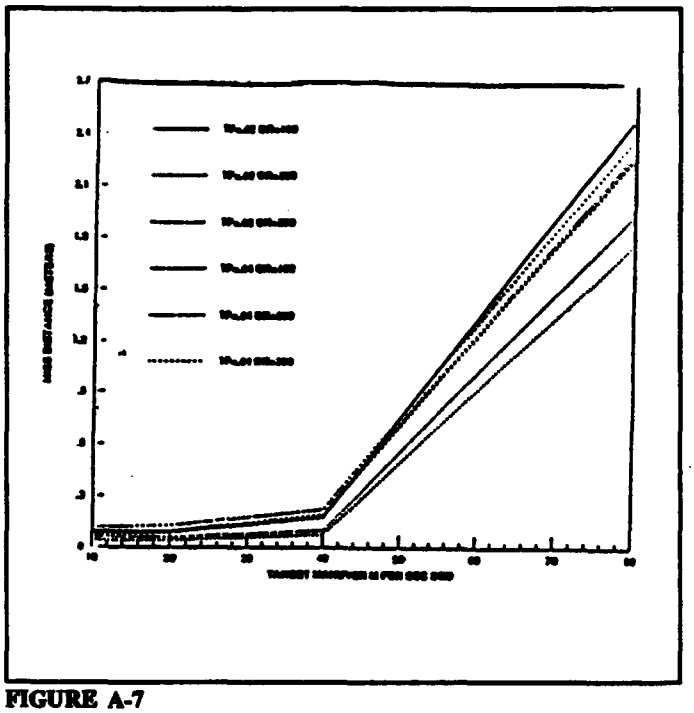

FIGURE A-7

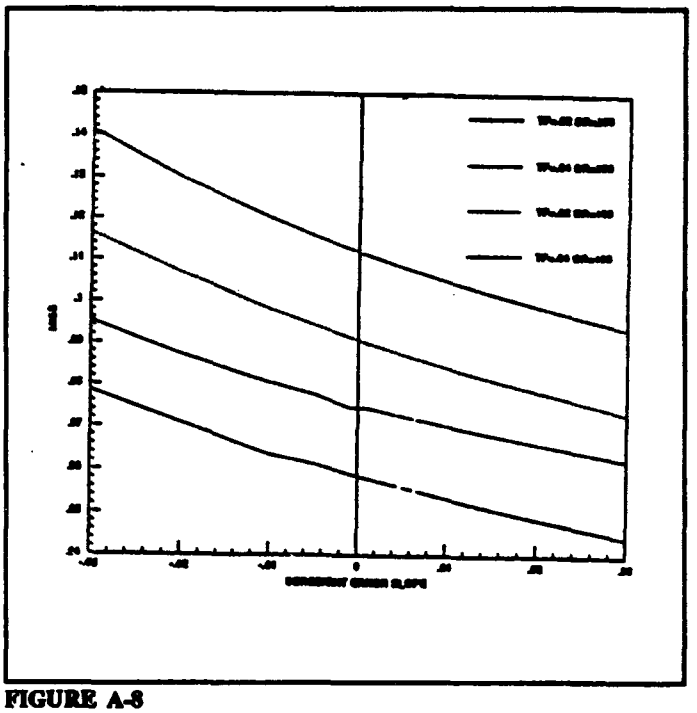

FIGURE A-8

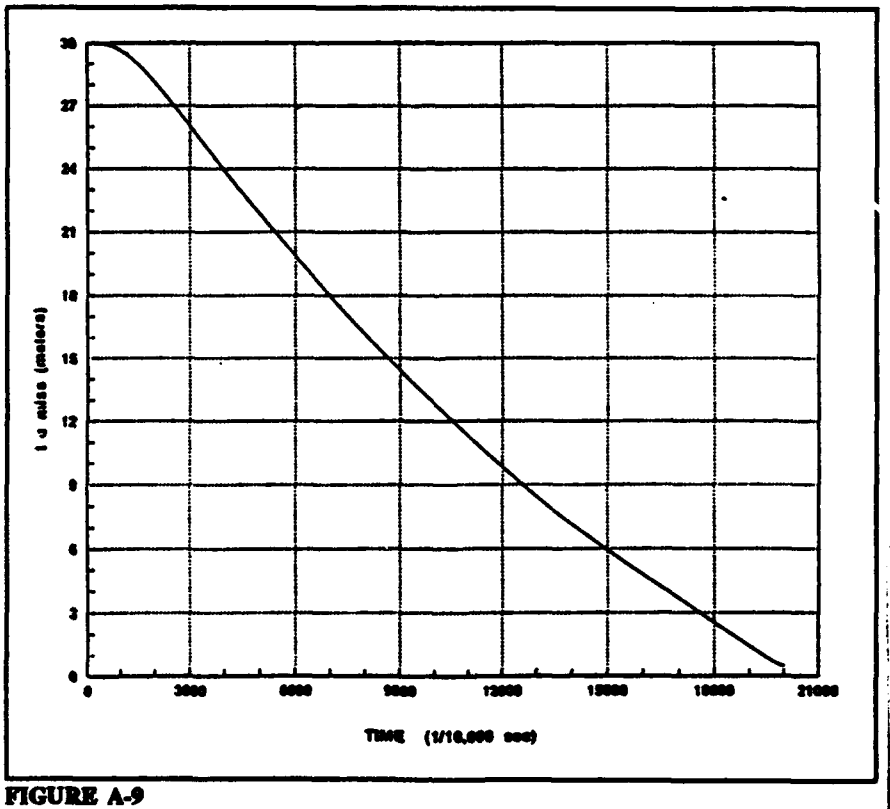

FIGURE A-9